

## COMPARATIVE STUDY BETWEEN CATALYST PROPERTIES OF SIMPLE SPINEL FERRITE POWDERS PREPARED BY SELF-COMBUSTION ROUTE\*

N. REZLESCU<sup>1</sup>, E. REZLESCU<sup>1</sup>, P.D. POPA<sup>1</sup>, C. DOROFTEI<sup>1,2</sup>, M. IGNAT<sup>1,3</sup>

<sup>1</sup> National Institute of Research and Development for Technical Physics, Iasi, Romania

<sup>2</sup> “Al. I. Cuza” University, Faculty of Physics, Iasi, Romania; docorneliu@yahoo.com

<sup>3</sup> Al. I. Cuza University, Faculty of Chemistry, Iasi, Romania

Received September 12, 2012

*Abstract.* Eight kinds of simple semiconducting spinel ferrites,  $\text{MeFe}_2\text{O}_4$ , were prepared by self-combustion method using nitrates as precursors. To determine the phase composition and the nanostructure characteristics were performed X-ray diffraction and SEM observations. EDAX spectroscopy was utilized to evaluate the chemical composition and BET analysis to determine the specific surface area. The ferrites have tested catalytically in combustion reaction of three diluted gases: acetone, ethanol and methanol. The results revealed a pronounced decrease in the combustion temperature when Mg-, Cu- and Ni- ferrites are used as catalysts.

*Key words:* ferrite, catalyst, self-combustion.

### 1. INTRODUCTION

High cost of noble metal catalysts imposes a need for developing alternative catalysts. Transition metal oxides are attractive alternatives due to their relatively low cost and earthly abundance [1–3]. The transition metal oxide catalysts are less active than noble metal catalysts, but more resistant towards catalyst poisoning. In the last years, nanograined oxide compounds, called ferrites, offer new opportunities for enhancing the performances of solid catalysts [4–8] due to the much higher surface to bulk ratio compared to coarse micrograined materials. High surface area of ferrites is priority for catalytic purposes. In general, high surface areas imply small particle sizes. The smaller is the particle size, the larger is the surface area, in front of gases for a given mass of particles. Hence, the control of morphology will be one of the first requirements for improving the catalyst activity. Ferrites are thermal and chemically stable ceramic materials, with low cost

\* Paper presented at the 8<sup>th</sup> General Conference of Balkan Physical Union, July 5–7, 2012, Constanța, Romania.

and easy processing. The conventional ceramic way for preparing ferrite powder does not allow a precise control of powder quality. For this reason, the researchers have tried new nonconventional procedures for preparing the spinel type ferrites with fine particles [9–13].

The purpose of this work was to find new ferrite compositions with suitable properties for catalyst applications.

## 2. EXPERIMENTAL

Eight kinds of simple spinel ferrites,  $\text{MeFe}_2\text{O}_4$  ( $\text{Me} = \text{Cu}, \text{Ni}, \text{Zn}, \text{Mg}, \text{Co}, \text{Ca}, \text{Li}$  and  $\text{Cd}$ ), were prepared by so called “self-combustion method” using nitrates as precursors [14]. Metal nitrates, ammonium hydroxide and polyvinyl alcohol were used as starting materials. Metal nitrates are the salts we preferred because they contain nitrogen and are water soluble (a good homogenization can be achieved in solution). Hydrate salts are even more favored, although the water molecules are irrelevant for the chemistry of the combustion. The preparation procedure by self-combustion is given in Fig. 1.

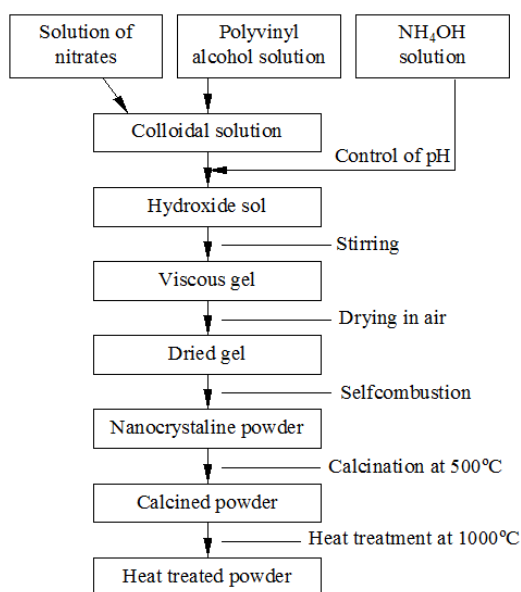


Fig. 1 – Processing of perovskite powders by self-combustion route.

This route included the following procedures: (1) dissolution of metal nitrates in deionized water; (2) polyvinyl alcohol addition to the first solution to make a colloidal solution; (3)  $\text{NH}_4\text{OH}$  addition to increase pH to about 8; (4) stirring at  $80^\circ\text{C}$ ; (5) drying the gel at  $120^\circ\text{C}$ ; (6) and finally self-combustion. The dried gel

was ignited at one end by using an electrically heated W wire (0.5 mm in diameter) and an exothermic combustion reaction began. The combustion front spontaneously autopropagates and converts the dried gel in a loose powder. The as burnt powders were calcined at 500°C for 30 min to eliminate any residual organic compounds. Then, calcined powders were heat treated at 900°C for a short time of 10 minutes, to obtain a good crystallinity of the powder without a sesizable increase of the crystallites.

The surface morphology has been analysed by a scanning electron microscope QUANTA 200 3D Dual Beam. The grain size was appreciated from SEM micrographs by linear intercept method [15]. The specific surface area (SBET) was determined by Brunauer-Emmet-Teller (BET) method [16] based on adsorption/desorption isotherms of nitrogen at 77 K obtained with NOVA 2200 apparatus. The pore size distribution (PSD) was calculated from the adsorption isotherms using BJH (Barrett-Joyner-Halenda) method [16]. The chemical composition of the surface particles was examined with an energy dispersive X-ray spectrometer (EDAX: Genesis). Incident electron beam energies from 0 to 14 KeV has been used. In all cases the beam was at normal incidence to the sample surface and the measurement time was 100 s. All the EDAX spectra were corrected by using ZAF correction which takes into account the influence of the matrix material on the obtained spectra.

### 3. RESULTS AND DISCUSSION

The X-ray powder diffraction was employed for phase identification and nanoparticle formation. The XRD patterns of the ferrite powders after heat treatment at 900°C are shown in Fig. 2 for two ferrites. Except for  $\text{CuFe}_2\text{O}_4$  ferrite, the cubic spinel phase formation with  $Fd3m$  space group was detected.  $\text{CuFe}_2\text{O}_4$  ferrite does not conserve cubic symmetry. This is a tetragonal distorted spinel (due to  $\text{Cu}^{2+}$  ions) with the space group  $I41/amd$ . The most intense peaks in all specimens are (220), (311), (400), (422), (333) and (440). Monophase crystalline materials were obtained.

From the results obtained by XRD analysis some observations can be made:

- the lattice constant depends on the Me type and suggests the formation of a compositionally homogeneous solid solution;
- the lattice constants for ferrite nanoparticles are close to those known for bulk ferrites;
- the crystallite size  $D_{\text{XRD}}$  calculated with Scherer's equation was found to be in the range 36 to 52 nm and this demonstrates that powders with nanosized crystallites have been obtained;
- though all samples were prepared under identical conditions, the crystallite size was not the same for all compositions; this increases with increasing the Me ion radius.

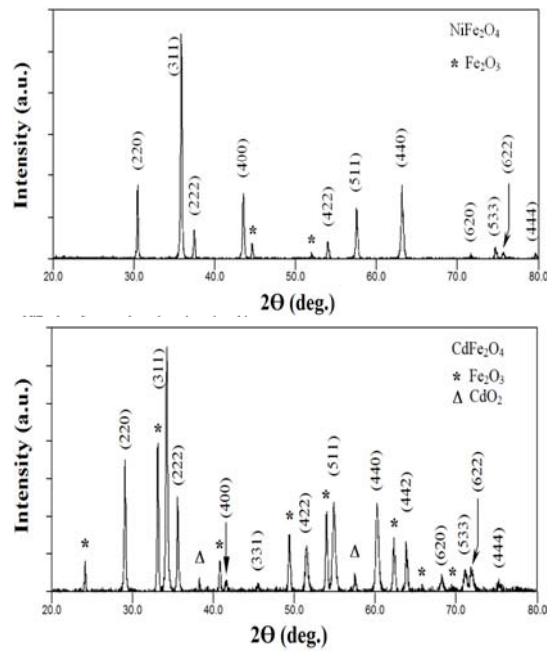


Fig. 2 – XRD patterns for two spinel ferrites ( $\text{NiFe}_2\text{O}_4$  and  $\text{CdFe}_2\text{O}_4$ ).

The surface morphology of the ferrite powders can be examined from SEM micrographs (Fig. 3). One can remark the high tendency of the fine crystallites to form mini- or macro-agglomerates having irregular shapes and sizes. The average size of the agglomerates estimated from these micrographs is between 400 nm and 550 nm. Large agglomerates dispersed through small agglomerates there are in Cd ferrite, of about 20 times as large as crystallites, due to the smallest crystallite size (33 nm). Agglomerates of approximately the same sizes are observed in other ferrites.

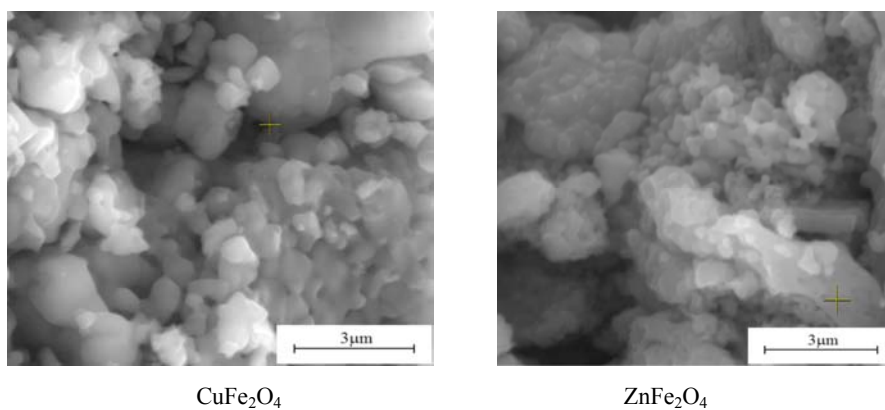


Fig. 3 – SEM micrographs for two spinel ferrites ( $\text{NiFe}_2\text{O}_4$  and  $\text{CdFe}_2\text{O}_4$ ).

The nitrogen adsorption/desorption isotherms at 77 K for  $\text{CuFe}_2\text{O}_4$  ferrite powder are shown in Fig. 4. One can see that the desorption branch does not follow the adsorption branch, but forms a distinct hysteresis loop because the amount adsorbed is greater along the desorption branch compared to the adsorption branch. The adsorption isotherms can be classified as type IV according to the IUPAC (International Union of Pure and Applied Chemistry) classification published in 1985 [16]. The hysteresis loop is of type H1. According to the IUPAC classification, type H1 is often associated with porous materials consisting of agglomerates of particles with approximately uniform spheres [16]. The inflexion point of isotherms indicates the stage at which monolayer coverage is complete and multilayer adsorption begins to occur.

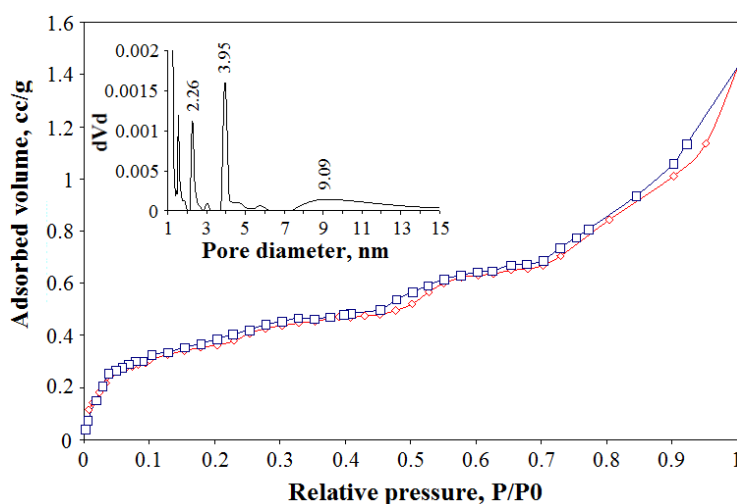


Fig. 4 – Nitrogen adsorption/desorption isotherms at 77K for  $\text{CuFe}_2\text{O}_4$  ferrite powder; symbol romb ( $\diamond$ ) is the adsorption branch and square symbol ( $\square$ ) is the desorption branch. Inset: the pore size distribution graphs.

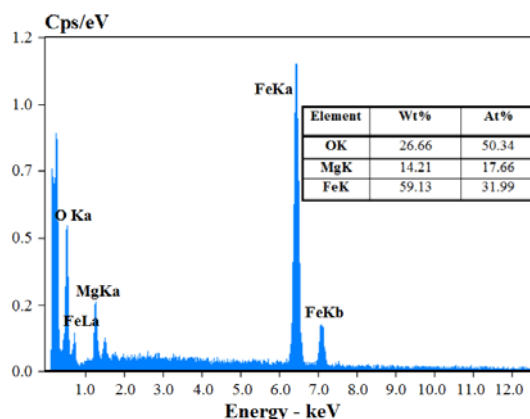
The BET surface area,  $S_{\text{BET}}$ , was evaluated from the nitrogen physisorption data using the Brunauer-Emmett-Teller equation [16]. All samples have reasonable specific surface area (see Table 1). Among all,  $\text{CdFe}_2\text{O}_4$  exhibits the smallest crystallite size (33 nm) and the higher specific surface area ( $4.75 \text{ m}^2/\text{g}$ ). The other samples have higher crystallite size and smaller specific surface area. From the adsorption/desorption branches of the isotherms were calculated the pore size distributions (PSD) by BJH method [16]. The PSD graphs are inserted in Fig. 4. One can remark that in the Cu- and Cd- ferrites there are two or three distinct pore size distributions, but all size ranges fall within the nanosized region. The BET surface area and pore volume for samples are given in Table 1.

Table 1

Powder characteristics of  $\text{MeFe}_2\text{O}_4$  ferrites

Samples	Average agglomerate size (nm)	$S_{\text{BET}}$ ( $\text{m}^2/\text{g}$ )	Pore volume ( $\text{cc/g}$ )
$\text{CuFe}_2\text{O}_4$	550	1.48	0.0020
$\text{NiFe}_2\text{O}_4$	500	3.86	0.0059
$\text{ZnFe}_2\text{O}_4$	600	3.00	0.0042
$\text{CdFe}_2\text{O}_4$	400	4.75	0.0060
$\text{CoFe}_2\text{O}_4$	350	3.26	0.0048
$\text{MgFe}_2\text{O}_4$	340	3.91	0.0060
$\text{LiFe}_5\text{O}_8$	450	2.77	0.0038
$\text{CaFe}_2\text{O}_4$	440	2.83	0.0049

The EDAX patterns confirm the homogeneous mixing of Mg, Li, Ca, Co, Zn, Ni, Cd, Cu and Fe atoms in samples and the purity of the chemical compositions. The Me/Fe molar ratio was found close to the theoretical value. EDAX spectrum for  $\text{MgFe}_2\text{O}_4$  powder is shown in Fig. 5. One can see characteristic peaks and the composition of  $\text{MgFe}_2\text{O}_4$  ferrite. The Mg/Fe molar ratio was found of 0.55, whereas theoretical value is of 0.5 which is a proof of homogeneous distribution of the elements in the solid.

Fig. 5 – EDAX spectrum for  $\text{MgFe}_2\text{O}_4$  ferrite.

The catalyst tests of the eight prepared ferrite powders were performed by measuring the minimum temperature at which the combustion reaction of very small concentrations of acetone, ethanol and methanol occurs in air environment catalyzed by ferrite powders. It is known that the catalyzed combustion reaction takes place at much lower temperatures than that non-catalyzed. In Fig. 6 the minimum temperature for combustion of the three diluted gases over the four ferrite nanopowders are given. For comparison is given also the minimum temperature required to ignite the mentioned gases without a spark or catalyst

being present. All experiments were conducted twice to ensure reproducibility; similar results were always obtained. In the bar diagram one can remark the change of minimum combustion temperature with ferrite catalyst composition. It is important to note that the most efficient ferrite catalyst is Mg-ferrite which has the greatest effect in decreasing the combustion temperature (to about 200 deg) of gases in air environment, being the most active catalyst.

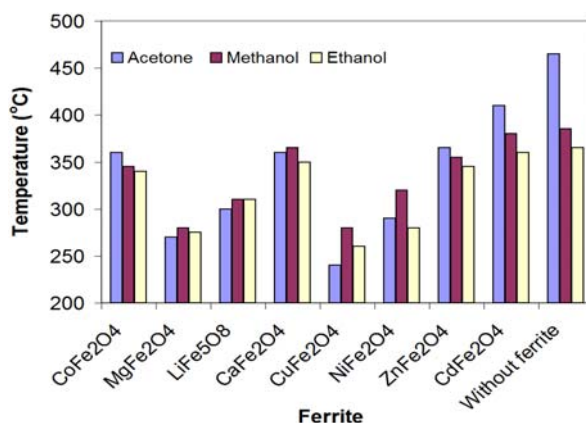


Fig. 6 – Bar diagram, for the minimum combustion temperature of acetone, ethanol and methanol vapor in air in the presence of ferrite catalysts and without catalyst.

It is known that the oxygen species ( $O^{2-}$ ,  $O_2^-$ ,  $O^-$ ) adsorbed on the oxide compound surface play a major role in the catalytic combustion [17–19]. The interaction of surface active oxygen species with reactants determines the mechanism for gas oxidation over mixed oxide catalysts, but the surface defects are sites for oxygen adsorption [20]. However, the possibility of involvement of the surface lattice oxygen in the gas combustion over mixed oxides cannot be excluded [21]. The valence of  $Mg^{2+}$ ,  $Li^+$ ,  $Ca^{2+}$  or  $Co^{2+}$  ions, lower than that of  $Fe^{3+}$  ion, can cause the formation of oxygen vacancies and modification of the lattice oxygen mobility.

In the present study, a possible explanation for the temperature differences in the gas combustion reactions catalyzed by various composition ferrites can be either different reactivity of the oxygen species adsorbed on the ferrite surfaces ( $O^-$  is more active than  $O^{2-}$ ) or various densities of the active surface sites. The improved activity of Mg containing ferrite can be mainly ascribed to a larger density of surface active oxygen species, weakly bonded on the ferrite surface, which can facilitate the ferrite to oxidize the combustible gas when this comes into contact with ferrite surface. Also, the larger surface area of Mg ferrite presumes much more intensive interactions between the ferrite surface and the gas which can promote the gas oxidation at lower temperatures. The weakly effect of Ca and Co ferrites suggests less active oxygen species available for the combustion reaction.

The obtained results incite to investigate also other ferrite compositions to find a catalytic material with the best properties.

#### 4. CONCLUSIONS

Spinel-type ferrite powders ( $\text{CoFe}_2\text{O}_4$ ,  $\text{MgFe}_2\text{O}_4$ ,  $\text{LiFe}_5\text{O}_8$ ,  $\text{CaFe}_2\text{O}_4$ ,  $\text{CuFe}_2\text{O}_4$ ,  $\text{NiFe}_2\text{O}_4$ ,  $\text{ZnFe}_2\text{O}_4$ ,  $\text{CdFe}_2\text{O}_4$ ) with nanosized crystallites were prepared by self-combustion method. The X-ray diffraction and SEM micrographs confirmed the presence of spinel phase as major phase, nanosize of the ferrite crystallites (33 – 52 nm) and the presence of the agglomerates. The catalytic tests showed that the catalytic combustion of the diluted gases (acetone, methanol and ethanol) when Cu, Mg or Ni spinel ferrite are used as catalyst can take place at much lower temperatures in comparison with normal combustion. A probable explanation for the better catalytic activity of these ferrites has been proposed. Experiments are under way to better understand the Ni-, Mg- and Cu- ferrite surface chemistry responsible for the observed performance.

**Acknowledgements.** This work was supported by a grant of the Romanian National Authority for Scientific Research, CNST – UEFISCDI, project number PN-II-ID-PCE-2011-3-0453.

#### REFERENCES

1. M.S. Sadjadi, M. Mozaffari, M. Enhessari, K. Zare, *Effects of NiTiO<sub>3</sub> nanoparticles supported by mesoporous MCM-41 on photoreduction of methylene blue under UV and visible light irradiation*, Superlattices and Microstructures, **47**, 685 (2010).
2. M. Epifani, E. Melissano, G. Pace, M. Schiopa, *Precursors for the combustion synthesis of metal oxides from the sol-gel processing of metal complexes*, J. Europ. Ceram. Soc., **27**, 115 (2007).
3. A.V. Murugan, V. Samuel, S.C. Navale, V. Ravi, *Phase evolution of NiTiO<sub>3</sub> prepared by coprecipitation method*, Materials Letters, **60**, 1791 (2006).
4. A.C.F.M. Costa, R.T. Lula, R.H.G.A. Kiminami, L.F.V. Gama, A.A. de Jesus, H.M.C. Andrade, *Preparation of nanostructured NiFe<sub>2</sub>O<sub>4</sub> catalysts by combustion reaction*, J. Mater. Sci., **41**, 4871 (2006).
5. D. Hirabayashi, T. Yosikawa, Y. Kawamoto, K. Mockizuki, K. Sukuki, *Characterization and Applications of Calcium Ferrites Based Materials Containing Active Oxygen Species*, Advances in Science and Technology, **45**, 2169 (2006).
6. N.L. Freitas, J.P. Continho, M.C. Silva, H.L. Lira, R.H.G.A. Kiminami, A.C.F.M. Costa, *Synthesis of Ni-Zn ferrite catalysts by combustion reaction using different fuels*, Materials Science Forum, **660–661**, 943 (2010).
7. J.C. Lou, C.K. Chang, *Catalytic oxidation of CO over a catalyst produced in the ferrite process*, Environmental Engineering Science, **23**, 1024 (2006).
8. Yunzhe Feng, Protap M. Rao, Dong Rip Kim, Xiaolin Zheng, *Methane oxidation over catalytic copper oxides nanowires*, Proceeding of the Combustion Institute, **33**, 3169 (2011).
9. D.H. Chen, X.R. He, *Synthesis of nickel ferrite nanoparticles by sol-gel method*, Mater. Res. Bull., **36**, 1369 (2001).

10. S. Prasad, N.S. Gajbhiye, *Magnetic studies of nanosized nickel ferrite particles synthesized by the citrate precursor technique*, J. Alloys Comp., **265**, 87 (1998).
11. A.C.F.M. Costa, E. Tortela, M.R. Morelli, R.H.G.A. Kiminami, *Ni-Zn ferrite nanoparticles prepared by combustion reaction*, Advanced Powder Technology III Book Series: Materials Science Forum, **416/418**, 699 (2003).
12. M. Tsuji, T. Kodama, T. Yoshida, Y. Kitayama, Y. Tamaura, *Preparation and CO<sub>2</sub> methanation activity of an ultrafine Ni(II) ferrite catalyst*, J. Catalysis, **164**, 315 (1996).
13. S. Komarneni, E. Fregeau, E. Breval, R. Roy, *Hydrothermal preparation of ultrafine ferrites and their sintering*, J. Am. Ceram. Soc. Commun., **71**, C26-C28 (1988).
14. P.D. Popa, N. Rezlescu, Gh. Iacob, *A new procedure for preparing ferrite powders*, Romanian Patent No.121300, OSIM, Bucharest, 2008.
15. M.I. Mendelson, *Average Grain Size in Polycrystalline Ceramics*, J. Amer. Ceram. Soc., **52**, 443 (1969).
16. S. Lowell, J.E. Shields, M.A. Thomas, M. Thommes, *Characterization of Porous Solids and Powders: Surface Area, Pore Size and Density*, Kluwer Academic Publishers, Dordrecht, Boston, London, 2004.
17. A. Machocki, T. Ioannides, B. Stasinska, W. Gac, G. Avgouropoulos, D. Delimaris, W. Grzegorzczuk, S. Pasieczna, *Manganese-lanthanum oxides modified with silver for the catalytic combustion of methane*, J. Catal., **227**, 282 (2004).
18. S.Q. Li, H.T. Liu, L.A. Yan, X.L. Wang, *Mn-substituted Ca-La-hexaaluminate nanoparticles for catalytic combustion of methane*, Catal. Commun., **8**, 237 (2007).
19. S.Q. Li, X.L. Wang, *The Ba-hemaluminate doped with CeO<sub>2</sub> nanoparticles for catalytic combustion of methane*, Catal. Commun., **8**, 410 (2007).
20. C. Li, K. Domen, K. Maruya, T. Onishi, *Dioxygen Adsorption on well-outgassed and partially reduced cerium oxide studied by FT-IR*, J. Am. Chem. Soc., **111**, 7683 (1989).
21. C. Laberty, P. Alphonse, J.J. Demai, C. Sarada, A. Rousset, *Synthesis and characterization of nonstoichiometric nickel manganite spinels  $NixMn_{3-x}$  square(3 delta/4) O-4+delta*, Mater. Res. Bull., **32**, 249 (1997).